Modelling of core molten material fast vaporisation and expansion for the evaluation of sfr severe accident consequences

A Mouly, N Seiler, F Bertrand, Michel Gradeck

The 19th International Topical Meeting on Nuclear Reactor Thermal Hydraulics (NURETH-19) Log nr.: 19001
Brussels, Belgium, March 6 - 11, 2022

MODELLING OF CORE MOLTEN MATERIAL FAST VAPORISATION AND EXPANSION FOR THE EVALUATION OF SFR SEVERE ACCIDENT CONSEQUENCES

A. MOULY, N. SEILER, and F. BERTRAND
CEA Cadarache
13108 Saint-Paul-lez-Durance, France
aude.mouly@cea.fr
nathalie.marie@cea.fr
frederic.bertrand@cea.fr

M. GRADECK
LEMTA, CNRS UMR 7563
University of Lorraine
CNRS, LEMTA, F-54000 Nancy, France
michel.gradeck@univ-lorraine.fr

ABSTRACT

The fourth generation of sodium fast reactors (SFR) is developed taking into account severe accidents as soon as the pre-conceptual phase is under way in order to increase safety margins. In this context, parametric and fast-running tools are used in addition to mechanistic tools during the reactor design phase for probabilistic margin evaluations.

The present paper is dedicated to preliminary transient modelling and studies of the expansion phase using a new parametric tool named MOREINa. Potentially occuring after a secondary power excursion in a SFR with low void worth core (non energetic primary phase), the expansion phase implies a vaporisation of superheated materials, their expansion and their interaction with the coolant, potentially jeopardizing the vessel mechanical integrity. MOREINa has a new expansion phase model considering both fuel and steel in order to evaluate the energy released during this secondary phase and its consequences on the reactor vessel structures.

This modelling, based on dimensional analysis and involving mass, momentum and energy balances, is done to simulate the vaporisation of two overheated liquids whose vapors supply a bubble of vapour and fission gases, the bubble expansion due to pressure difference between the bubble and the cover gas located at the top of the vessel and finally the FCI induced by thermohydraulic instabilities and contributing to the further fragmentation of the molten materials. The energy released is evaluated to assess order of magnitudes of the mechanical loading applied on the reactor vessel. Comparison with a CEA validated parametric tool DETONa are finally presented and analyzed.

KEYWORDS
SFR, severe accidents, expansion phase, dimensional analysis, MOREINa

1. INTRODUCTION

Improving reactors technology in order to excel safety and reliability at industrial scale is one of the current objectives of the fourth generation of nuclear reactors (GEN IV). Among the six nuclear concepts of this generation, Sodium Fast Reactor (SFR) has been selected for its ability to sustainably manage radioactive

waste and nuclear fuel ressource [1]. This neutron fast reactor concept is well known in France because of previous fast reactors feedback (Rapsodie, Phenix and Superphenix). At CEA, further developments of SFR are conducted in the scope of safety standard of the GEN IV. Thus, taking into account hypothetical severe accidents involving the melt down of the reactor's core is required in the safety analyses during the preconceptual phase.

Severe accidents are studied in the safety analysis of design phase by using two different approaches [2] : the deterministic approach and the probabilistic approach. The first approach uses unfavourable scenario to demonstrate the compliance of the reactors to safety requirement and verify the margins regarding the safety criteria. Complex mechanistic codes are used such as SIMMER and EUROPLEXUS during this approach.

The second one studies the behaviour of the reactor with different scenarios using the occurrence probabilities of phenomena (Best Estimate Plus Uncertainties method). This approach is more appropriate to calculate safety margin probabilities. Other codes are needed in this second approach owing to the high CPU time of the complex mechanistic codes which prevent their use from such probabilistic studies. In this context, the R&D progress in CEA provided fast-running tools in order to evaluate safety margins, uncertainties studies and parametric studies. The present paper is dedicated to the presentation of one of them, named MOREINa*. This tool models a part of the expansion phase which is a specific phase of severe accidents in SFR.

In this paper, we detail the modelling and we also present first results. At first, the expansion phase will be described. Then, the physical modelling will be detailed. In a second time preliminary results and preliminary sensitivity studies will be shown and analyse. Finally, a comparison with a validated parametric tool will be presented.

2. THE EXPANSION PHASE

The expansion phase during a SFR severe accident is a highly hypothetical situation studied in the reactor preconceptual phase in order to achieve safety requirements. It can potentially occur in SFR severe accident when molten materials are forming pools in the internal structures of the vessel.

This phase begins when the pool composed by the core molten materials undergoes a recriticality induced by its compaction. This pool recriticality involves a secondary power excursion, implying an increase of the pool temperature. If the pressure of the pool is lower than the increasing saturation pressure obtained with a correlation on the saturated temperature of the liquid materials, the molten materials vaporisation begins by flashing and creates a bubble of vapour. The pressure difference between the bubble vapour and the reactor's cover gaz initiates an expansion of the vapour towards the cover gas in the mechanism.

Because of the thermal equilibrium break up during the expansion of the vapour bubble by vapour pressure decrease, the pool vaporises and supplies the bubble to reach another thermal equilibrium between the vapour and the liquid. The bubble expansion can also potentially induce instabilities which can promote fragmentation between the different fluid layers. These instabilities are driven by the density difference between the fluid layers and the velocity of the vapour expansion.

Furthermore, if the expansion leads the liquid molten core materials into the sodium, a fuel coolant

*MOdel of vapouR Expansion and fuel coolant Interaction in Natrium

interaction can also occur and induce Sodium vaporisation and the resulting bubble expansion. The mechanical energy released by the vaporisations, expansions and interaction will potentially jeopardize the reactor vessel structure (see figure 1).

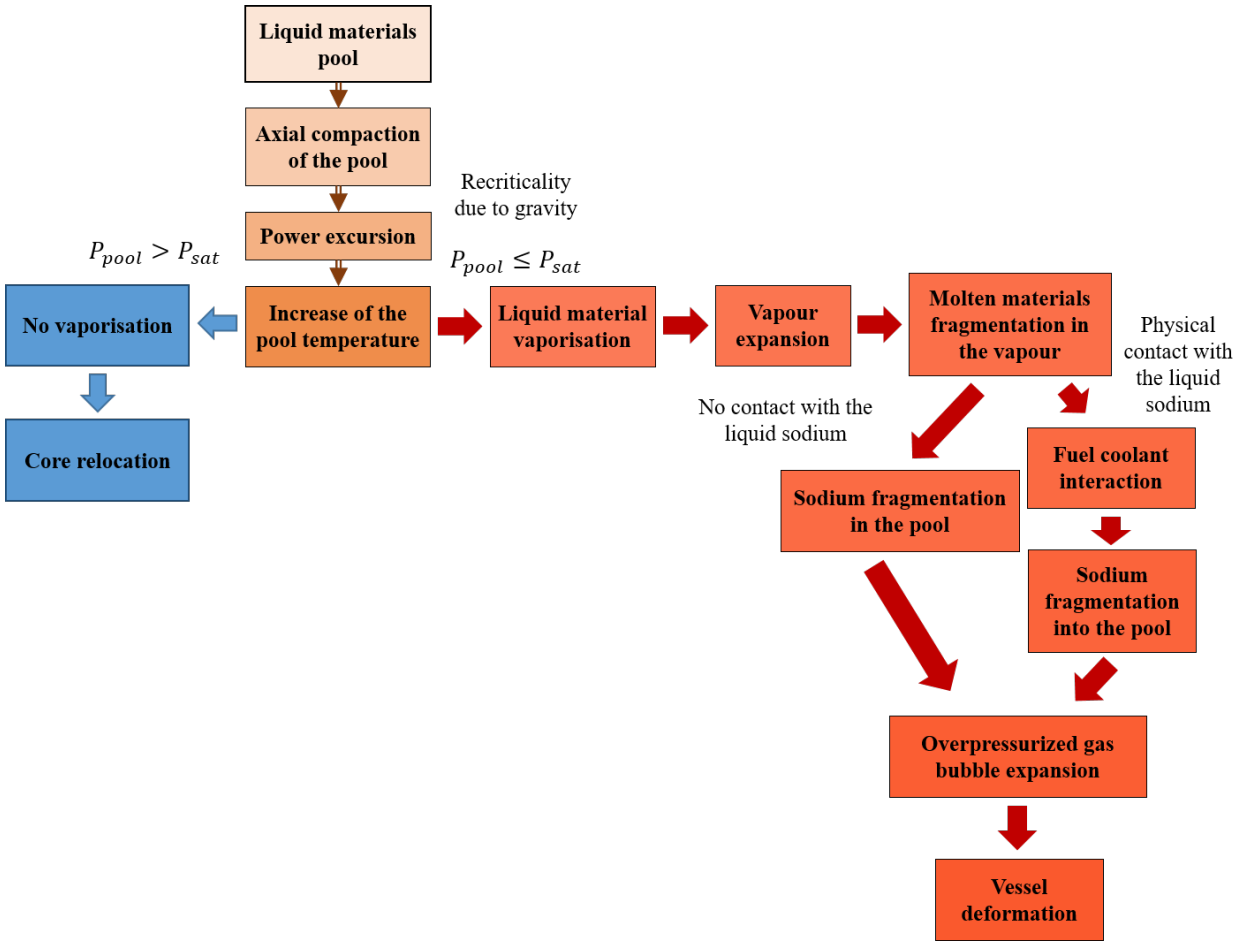

Figure 1. Phenomenological tree of the expansion phase

3. DESCRIPTION OF THE PHYSICAL MODELLING

The models implemented in MOREINa describe the vaporisation of superheated molten materials in the internal structures of the core and the expansion of the generated vapours forming a bubble because of the pressure difference with the upper cover gas.

3.1. Main assumptions

In MOREINa, the studied system is considered adiabatic. This is justified because four order of magnitude are separating the lost energy from lateral wall to the thermal energy of the pool during the transient. Moreover, the pool is supposed to be non compressible. The initial superheated liquid materials are

assumed to be composed of liquid steel, liquid fuel and fission gases. The non missibility of the liquid steel in the liquid fuel involves liquid steel bulks homogeneously distributed in the liquid fuel.

The distribution of temperature is parabolic along the z axis with the hotest part at the center of the liquid pool materials because the power excursion is driven by the neutron flux in the pool. At the uppermost location, the non liquid part of the core is full of Argon gas (see figure 2). This modelling is an academic case and has been chosen to study the behaviour of the molten materials vaporisation and vapour bubble expansion. The sodium will be included in MOREINa, between the pool and the argon gas, in further developments.

At the initial time, the metastable state of the pool is assumed to break and vapour production is beginning to reach a stable state. Argon gas and the fission gases are supposed to be perfect gases and their evolution is assumed to be isentropic.

3.2. Tool characteristics

MOREINa is a 0D multi-area explicit sheme calculation tool whose equations are solved using the fourth order of Runge-Kutta calcultation method (RK4).

In the calculation tool, the core modelling is developped considering a cylindrical geometry in which the vapour bubble evolution is supposed to be planar. This configuration has been chosen to fit with the geometry of the reactor core. A mesh grid is implemented along the height of the core in order to discretize the temperature and the mass in the core (see figure 2).

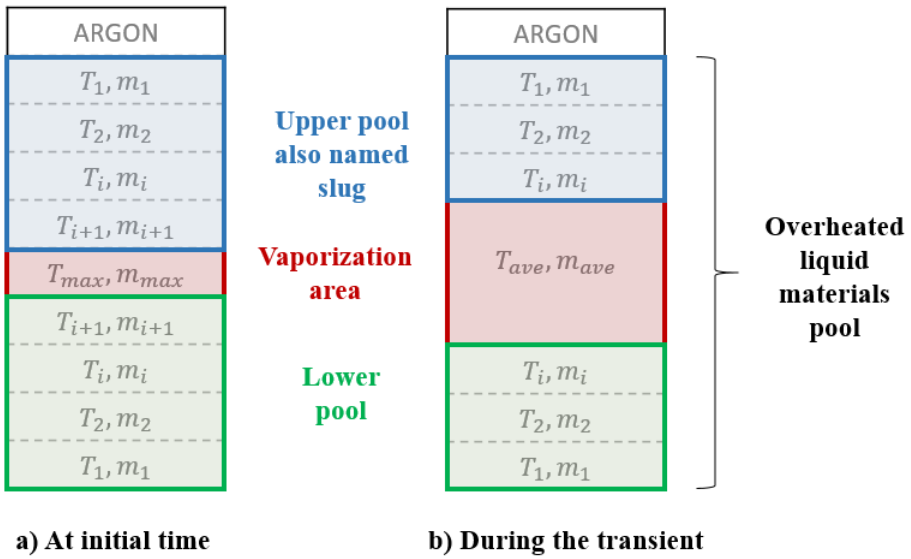

Figure 2. Mesh grid scheme implemented in MOREINa

This calculation tool is considered as a 0D multi-area tool because the balance equations constituting the modelling are applied on different zones of the pool. One zone is defined by one or more meshes,

depending on the transient evolution. The first zone is the molten materials above the vapour bubble also cited as slug (see the blue part in the figure 2). The second one is named the vaporisation zone (see the red part in the figure 2) and corresponds to the mesh(es) with the higher temperature at initial time. Finally the last one in the system covers the molten materials below the vapour bubble (the green part in the figure 2).

The different areas defined at initial time evolve during the transient because of the molten pool materials vaporisation (see figure 2, b). Indeed, the temperature in this zone decreases as the pool vaporises. The adjacent meshes are included in the vaporized area when the temperatures of the meshes become equal (see figure 2, b).

The vapour formed during the transient supplies one unique bubble in which the fission gases, the steel vapour and the fuel vapour are mixed. This bubble is considered to be at the hotest part of the mesh, in the middle of the vaporisation zone throughout the transient.

3.3. Major phenomena

The bubble expansion of the modelling is decribed by a momentum balance equation applied on the liquid above the vapour, the slug.

$$\boxed{\frac{\partial \dot{z_1}(t)}{\partial t} = \frac{1}{(z_{pool}(t) - z_1(t))} \frac{P_{bubble} - P_{Ar}(t)}{\rho^l_{pool}} - g} \tag{1}$$

Where z_1 is the upper vapour/liquid interface elevation and z_{pool} the liquid/Argon interface elevation. g is the gravity acceleration and ρ^l_b is the density of the pool above the bubble. The Argon pressure $P_{Ar}(t)$ and the fission gasses pressure P_{GF} are calculated using Laplace's law for diatomic gases. The global vapour pressure of the bubble P_{bubble} is calculated using Dalton's law and Raoult's law by adding partial pressures obtained with the saturation pressure and the steel mole fraction in the pool for the liquids (y_s). P_{GF} is calculated with Laplace's law for fission gases.

$$P_{bubble} = y_s P_s^{sat}(T^{sat}) + (1 - y_s) P_f^{sat}(T^{sat})) + P_{GF} \tag{2}$$

The molten materials vaporisation has been separately modelled between the two superheated molten materials, fuel and steel, to treat the non-miscibility of the dedicated liquids. For each liquid, a system to solve has been expressed using two balance equations.

First, the enthalpy balance equations have been expressed using thermal properties and vapour mass fraction for the dedicated liquids (see the first equation line in the system 3). The second equation is the derivated mass balance expressing the two-phase flow volume with the vapour density ρ_v, the liquid density ρ_l and the vapour mass fraction x (see the second equation line in the system 3). The liquid volume change has been neglected because of the low order of magnitude difference with the vapour volume change (n is representing the studied liquid, either fuel or steel).

$$\begin{cases} m_n \left[\left(x_n \dfrac{dh_v^n}{dT_n^{sat}} + (1-x_n) \dfrac{dh_l^n}{dT_n^{sat}} - \dfrac{V_n^{tot}}{m_n} \dfrac{dP_n^{sat}}{dT_n^{sat}} \right) \dfrac{dT_n^{sat}}{dt} + \Delta h_{l,v}^n \dfrac{dx_n}{dt} \right] = & \dfrac{dQ_n}{dt} \\ m_n \left[\dfrac{dx_n}{dt} \left(\dfrac{1}{\rho_v^n} - \dfrac{1}{\rho_l^n} \right) + \left(x_n \dfrac{\partial(1/\rho_v^n)}{\partial T_n^{sat}} + (1-x_n) \dfrac{\partial(1/\rho_l^n)}{\partial T_n^{sat}} \right) \dfrac{dT_n^{sat}}{dt} \right] = & \dfrac{dV^v}{dt} \end{cases} \tag{3}$$

Being included in one unique pool, a conducto-convective heat transfert ($Q_s = -Q_f$) has been implemented between the liquid steel and the liquid fuel. Having unknown bulks of steel in the fuel vapour, the heat exchange surface has been maximised resulting from stable droplets of steel in the fuel whose limit size is given by the critical Weber number ($We_c = 12.$).

$$\frac{dQ_s}{dt} = -\frac{dQ_f}{dt} = hS_{ech}\Delta T = hS_{ech}(T_s^{sat} - T_f^{sat}). \tag{4}$$

In order to verify the consistency of the mass and energy exchanges during the transient, the mechanical energy and a mass balance are calculated. The mechanical energy balance is described by the four energies involved during the transient ; the expansion energy, the compression energy, the kinetic energy and finally the potential energy (Equation 5).

$$E_{expansion} = E_{compression} + E_{kinetic} + E_{potential} \tag{5}$$

The expansion energy, $E_{expansion}$, is the energy released by the vapour bubble expansion, especially the pressure and volume vapour bubble evolution. The compression energy, $E_{compression}$, represents the energy of the Argon compression, is also calculated with the pressure and volume evolution of the Argon gas. The kinetic energy, $E_{kinetic}$, is the energy induced by the slug motion and finally, the potential energy, $E_{potential}$, is also the energy calculated by the slug evolution inside the core.

3.4. Instabilities located at the upper vapour/liquid interface

The vapours bubble expansion and the density difference between the liquids and the vapours involves Rayleigh-Taylor (RT) instabilities at the liquid/vapour interface during the transient (see figure 3). Due to these instabilities, molten materials jets from the slug are created and liquid droplets may be included in the vapour according to jet break up during the transient. To take into account this phenomenon, a model dealing with droplets production in the vapour has been implemented in MOREINa.

Rayleigh-Taylor instabilities in MOREINa's modelling are described in figure 3. The slug is represented in orange and the vapour driving the liquid during the expansion is represented in blue. The perturbations, induced by RT instabilities, are sinusoidal perturbations and only the most unstables ones leading to droplet formation are modelled. The most unstable wavelength is calculated using the cut-off wavelength, defined as the wavelength above which the perturbations becomes unstables and start to growth (Equation 6).

$$\lambda_{RT}^M(t) = \sqrt{3} \times \lambda_{RT}^c(t) = \sqrt{3} \times 2\pi \sqrt{\frac{\sigma_{pool}}{(\rho_{pool}^l(t) - \rho_{bubble}^v(t))\ddot{z}_1(t)}}. \tag{6}$$

Jets induced by the perturbations growth are supposed to be homogeneously distributed at the bubble interface. Experiences have showed an hexagonal distribution pattern [3] with the most probable wavelength of the RT instabilities as the period of the hexagon. Thus, the jet density per unit surface is calculated as a function of the wavelength and the mean number of jets in an hexagonal mesh.

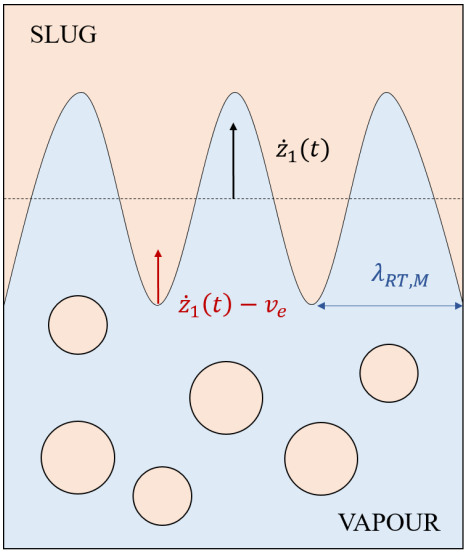

Figure 3. Droplet creation and inclusion scheme in MOREINa

The jets created by RT instabilities are growing during the transient. The rate of the jet growth has been studied with experiments [4] showing that it reaches an asymptotical speed. Two different correlations from different works [5] [6] have been implemented into the model at user's convenience. The first one, also named Corradini's velocity, expresses the velocity with the local scale of the system, the most unstable wavelength. The second one, named Lainault's velocity, expresses the velocity using the local and the global scale of the system, the vessel diameter and also the most unstable wavelength.

$$v_e = K\sqrt{\lambda_{RT}^{C}\ddot{z}_1} \tag{7}$$

$$v_e = \alpha_1 \left(\ddot{z}_1 \lambda_{RT}^{c}\right)^n + \alpha_2 \left(\ddot{z}_1 D_T\right)^m \tag{8}$$

Where $K = 4.65$, $\alpha_1 = 2.3$, $\alpha_2 = 0.35$, $n = 0.28$ and $m = 0.4$.

Jets breaks up and droplet creation are well known as the fragmentation process. In MOREINa, the main fragmentation regime is a transient turbulent regime involving a combination of Kelvin-Helmholtz instabilities, Rayleigh-Taylor instabilities and capillarity forces to create the droplets [7]. Due to the modelling choices in MOREINa, the flow evolution cannot be locally described around the perturbations. Then, the jet breakup implying spherical droplets creation has been postulated to occur when the length of the jet is above $\lambda_{RT}^{M}(t)$. The spherical droplets diameter is considered equal to $d_{drop} = \lambda_{RT}^{M}(t)/2$ [8] (see figure 3).

Droplets' families are created each time jets are fragmented during the transient. The families are divided into two parts, fuel droplet and steel droplets features, each one depending on the fragmentation time.

A second type of fragmentation is also considered in the modelling in order to take into account the fragmentation of the created droplet in the vapour flow due to the competition between the flow inertia force and the droplet surface tension force. A simple model has been implemented involving the comparison of the droplet Weber number and the critical Weber number.

3.5. Thermal evolution of the droplets in the vapour

Because of the axial distribution of the pool temperature, droplets created by fragmentation process and included in the vapour bubble have a different temperature than the vapour in the vaporisation area. Thus, heat transfers between the two phases must be modelled because it can potentially involve phase changes : droplet partial or total vaporisation and vapour condensation on the droplet surface.

Thermal evolutions of created droplets have been implemented in MOREINa by evaluating two total heat transfers, one for each liquid fluid. This total heat transfer is calculated by summing each transfers between the droplets of corresponding part of the family (steel or fuel) and the vapour bubble. For each part of the family, the conducto-convective and radiative heat transfers are considered and calculated in order to evaluate the temperature evolution of the droplets integrated in the vapour.

$$\frac{dQ_{i,j}}{dt} = \frac{dQ_{i,j}^{rad}}{dt} + \frac{dQ_{i,j}^{conv}}{dt} = S_{i,j}\varphi_{i,j}(T_{vapour} - T_{i,j}) + S_{i,j}\epsilon_{i,j}\nu(T_{vapour}^4 - T_{i,j}^4). \tag{9}$$

The index i corresponds to the family's number and the index j represents the steel or fuel part in the family. Furthermore, $S_{i,j}$ is the heat exchange surface calculated by summing all the droplets surfaces and $h_{i,j}$, the heat exchange coefficient between the vapour bubble and the droplets. The averaged temperature of the vapour is named T_{vapour} and $T_{i,j}$ corresponds to the droplet's temperature. ν is the Boltzmann constant and finally, $\epsilon_{i,j}$ is the liquid absorbtivity.

The temperature of the droplets is updated using the calculated heat exchange and compared to the saturated temperature of the corresponding liquid. If the obtained temperature is higher than the saturated one, vaporisation is simulated. The vaporised mass is calculated using an enthalpy balance equation and droplets are partialy or totally vaporised. If the updated temperature is smaller than the saturated temperature, no vaporisation is considered and the heat exchange heats up the droplets.

The total heat exchanges are finally added to the vaporisation systems as a source in the enthalpy equation to integrate the potential vapour condensation on the droplets surface.

4. PRELIMINARY RESULTS

Preliminary results have been obtained with MOREINa. This academic case has been developped to study and verify this first part of the expansion phase modelling : pool vaporisation and vapour expansion in the core.

4.1. Reference case

This case has been computed without integrating instabilities at the upper vapour-liquid interface. The different parameters used for the calculation of this reference case are summarised in the followed table. The meshgrid chosen for the computation is composed of 1000 meshes and the temperature difference between the hotest part of the meshgrid and the lowest is $\Delta T = 5446 - 3700 = 746K$. Meshgrid sensitivity studies on the time of discretisation have highlighted the value 10^{-6} s as the most adapted time of discretisation for this transient.

Table I. Calculation initial parameters of the reference case

Parameters	Unit	Value
Core internal structures height	m	1.5
Core internal structures radius	m	1.7
Total pool mass	t	40000
Steel mass fraction in the pool	-	0.3
Argon pressure	Pa	1.12×10^5
Argon volume	m^3	6.1
Fission gases pressure	Pa	33.44×10^5
Fission gases volume	m^3	5.15×10^{-3}

The results (see figure 4) show the evolution of the relevant variables during the transient. 52 kg of liquids are vaporised during the transient. This molten materials vaporisation induces a 200 K decrease of the temperature. The fuel temperature decrease is higher than the steel temperature decrease (around 50 K) because of the smaller value of fuel latent heat of vaporisation than steel latent heat of vaporisation. This difference involves an higher fuel mass vaporisation than steel one.

The pressure difference between the vapour bubble pressure and the Argon pressure generates an increase of the upper vapour/liquid interface velocity until 44 m/s and an increase of the corresponding height $z_1(t)$. The acceleration evolves due to the pressure difference and the liquid mass above the vapour. The more the vapour pression decreases, the more the acceleration decreases. When it reaches negative values, the velocity decreases until the system finds a stable state and the transient ends. The vapour pressure has an high value (17 MPa) at initial time because of the fission gases and decreases with the expansion to reach 9.8 MPa. The Argon pressure is increasing during the transient due to the expansion of the vapour volume and the decrease of the argon volume.

During the transient, the mechanical energies are highlighting the explained phenomenon : the expansion energy grows proportionnaly to the vapour volume evolution due to the vaporisation of the liquids. The compression energy increases because of the argon pressure increase induced by the expansion of the vapour and finally the kinetic energy follows the upper vapour/liquid interface velocity during the transient. Furthermore, the expansion energy is at the final state equal to the Argon compression energy. This demonstrates no energy loss during the transient and validates the numerical implementation in MOREINa.

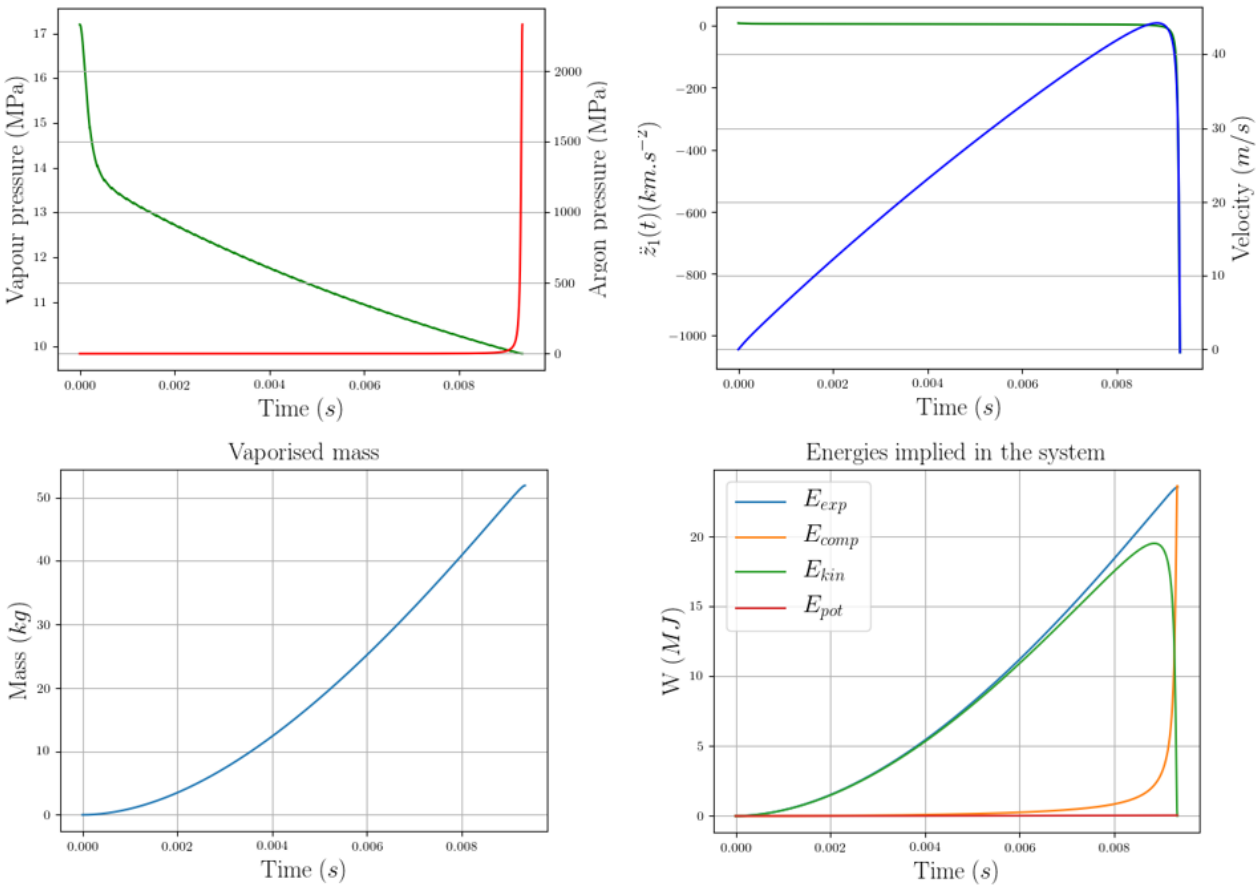

Figure 4. Relevant values during the MOREINa's transient

4.2. Taking into account instabilities

The results presented in this part are performed with the instability models implemented in MOREINa considering the jets growth rate expressed with the local and the global scale of the system, the Lainault velocity [6] (Equation 8).

The results (see figure 5) are similar as the reference case where no instability is taken into account until $0.004\ s$, the beginning of the droplets inclusion inside the vapour. $470\ kg$ of fuel droplets and $170\ kg$ of steel droplets are included inside the vapour bubble during the transient. The vaporised mass of the droplet is almost totally coming from the fuel droplets because of the fuel latent heat vaporisation smaller than the steel one. $33\ kg$ of fuel under the form of droplets are vaporised during the transient which impacts the vapour pressure and the fuel temperature. The vapour pressure increases around $0.005\ s$ because of the higher amount of vapour formed during the transient. High thermal exchanges are implemented between the vapour and the droplets created by fragmentation which induce an important decrease of the difference between fuel and steel temperature in this case.

Furthermore, the upper vapour/interface velocity reaches an higher maximun (3 %) due to the loss of mass in the slug by droplets inclusions. Because of this higher interface velocity and the more vaporised mass during the transient, the Argon pressure is also higher (16 %).

Finally, the mechanical energies implies in this transient are 5 % higher than the mechanical energies calculated in the reference case because of the implied vaporisation and the more important induced global bubble vapor during the transient.

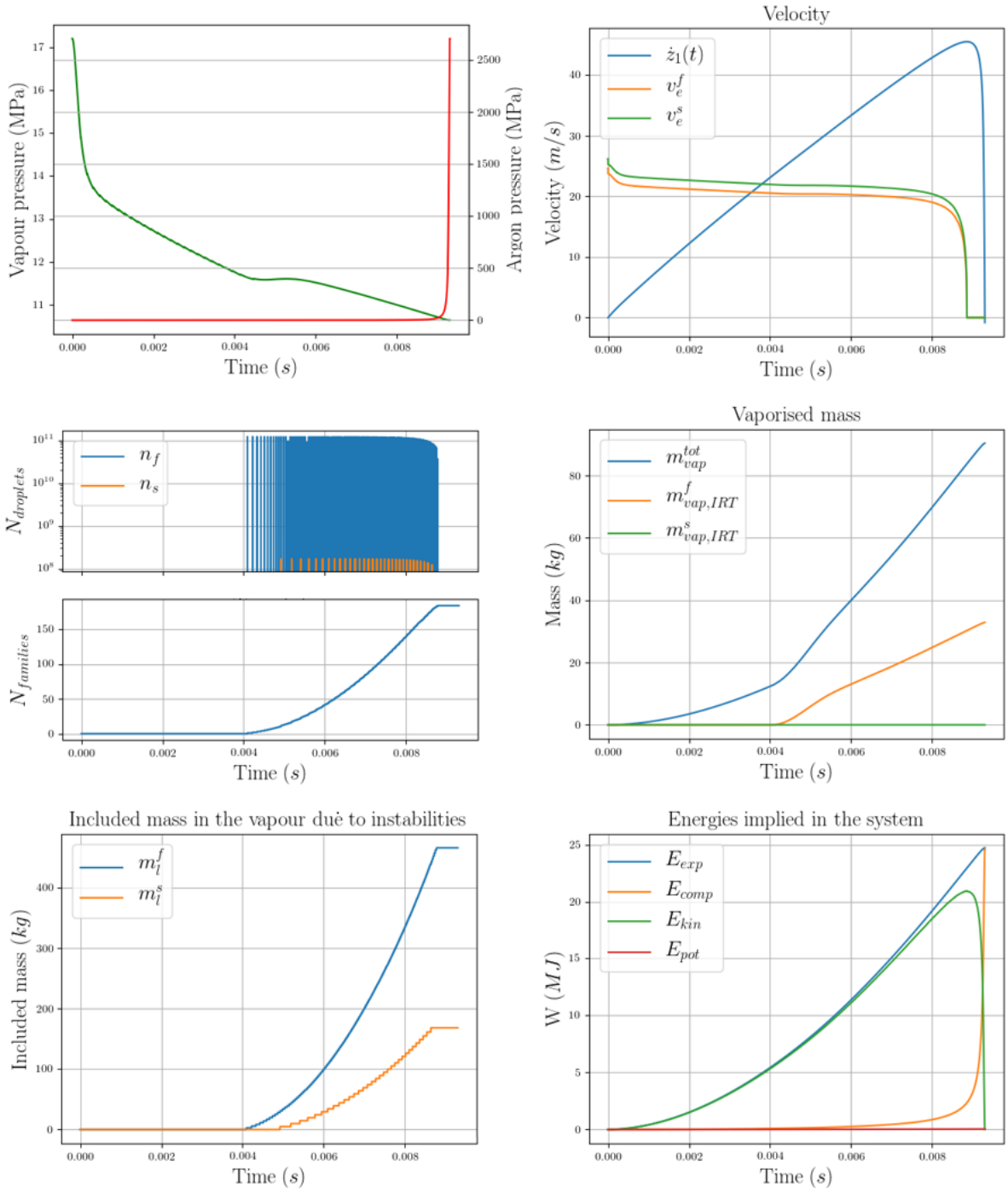

Figure 5. Relevant values during the MOREINa's transient with instabilities

5. COMPARISON TO THE DETONA PARAMETRICAL TOOL

The DETONa parametrical tool was developped by Xavier Manchon [8] to model the fuel vaporization and a global bubble expansion in a SFR. DETONa focuses on the mechanical energy released by the fuel vapour expansion pushing away the sodium phase towards the vessel structures. This code is computed in a spherical geometry and implies the presence of a sodium liquid column around the fuel pool (see figure 6). No interaction between the fuel and the sodium are modelled and the vapour formed is supposed to be between the fuel pool and the sodium around. An Argon phase is also simulated in order to represent the core cover gas. This parametric tool has been validated on experiments.

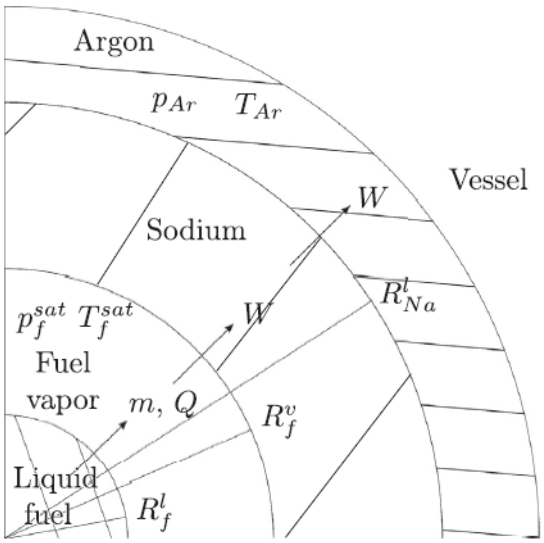

Figure 6. Modeled geometry in DETONa [8]

Comparing MOREINa's results to DETONa's results is interesting to assess relevancy of MOREINa's results. For the comparison, some adaptations have been performed in MOREINa :

- A sodium column has been implemented above the melted pool ;
- Steel and fissions products have been eliminated from the pool for the comparison calculation ;
- The vessel volume has been adapted to cope with DETONa's vessel volume.

Because of the two different geometries, spherical geometrie in DETONa modelling and cylindrical geometrie in MOREINa modelling, the results are expected to be the same order of magnitude but small discrepancies are expected. The parameters used for this comparison are resumed in the followed table (Table II).

Table II. Calculation parameters of the reference case

Physical parameters	Unit	Value
Total pool mass	t	40000
Pool temperature	K	5000
Steel mass fraction in the pool	-	0
Argon pressure	Pa	1.12×10^5
Argon volume	m^3	6.1

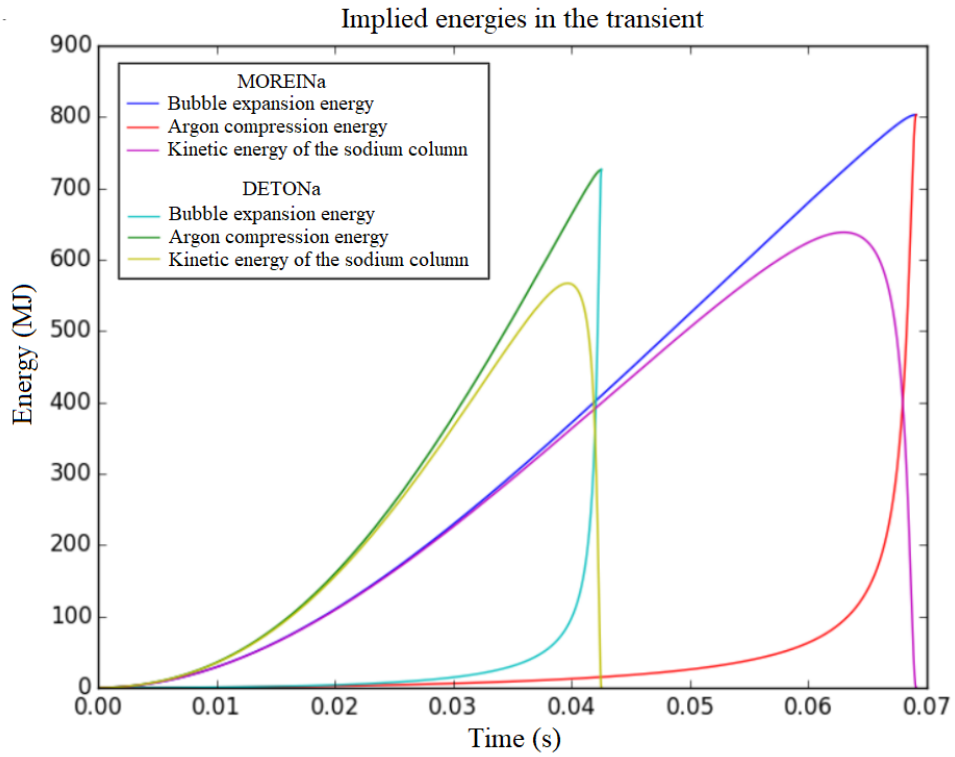

Figure 7. Mechanical energies comparison between MOREINa's transient and DETONa's transient

The energies involved in the two transient have the same order of magniture (figure 7). The expansion energy and the compression one calculated at the end of MOREINa's transient admit a 7 % deviation compared with DETONa final energies. This gap, also found on the vaporised fuel mass (7%) and the temperature (2%) due to the geometry difference between the two models. In the spherical geometry, the pressure is applied on a section evolving with the bubble expansion during the transient. On the contrary, in the cylindrical geometry the pressure section is constant. This geometrical feature impacts the momentum equation and the pool vaporisation.

Furthermore, the two transients have an important temporal gap : MOREINa's transient is around 0.07 s while DETONa's transient is around 0.042 s. This gap can be explained by the expansion time.

To obtain the expansion time δt^2_{exp}, the momentum equation is applied to DETONa's spherical volume. The sodium radius evolution is assumed to be enough small to be neglected face to the bubble radius

evolution and the acceleration is approximated by $R/\delta t_{exp}^2$.

$$\delta t_{exp}^{DETONa} = R_{bubble}\sqrt{\frac{\rho_{Na}^{l}}{3(P_{bubble} - P_{Ar})}} = 0.048s \tag{10}$$

By applying the same equation to MOREINa's system, the expansion time expression is obtained.

$$\delta t_{exp}^{MOREINa} = Z_1\sqrt{\frac{\rho_{Na}^{l}}{P_{bubble} - P_{Ar}}} = 0.067s \tag{11}$$

The $\frac{1}{\sqrt{3}}$ in the expression of DETONa's characteristic time (Equation 10) originate from the difference between the volume and the surface in a spherical geometry.

The two different expressions of the expansion time underscore the time-gap between the two modelling. To conclude, the comparison of the fuel vapour expansion results between MOREINa and DETONa allows to validate the order of magnitude of the model and the gap obtained between the two geometries were expected.

6. CONCLUSION

In the scope of the safety standards of the GEN IV, a modelling of the vaporisation and the expansion of the formed vapour have been developped and implemented in a fast-running tool. The preliminary results obtained from a transient study of this first part of the expansion phase modelling have been presented. Two differents results have been analyzed, one without taking account instabilities and another one taking account this phenomenon. Finally a comparison with a validated tool, DETONa have also been conducted for the fuel vaporisation and expansion modelling. Further developments will focus on the sodium interaction phenomenon after the expansion phase to evaluate the total loadings applied on the second barrier (i.e the vessel).

ACKNOWLEDGMENTS

The autors would like to thanks CEA's Generation IV SFRAG project, which suports this study.

NOMENCLATURE

Symbols		*Subscripts/Superscripts*	
$z[m]$	Height	$Ar[-]$	Argon
$\dot{z}[m]$	Height time-derivative	$pool[-]$	Pool
$\ddot{z}[m]$	Height second time-derivative	$1[-]$	Upper vapour/liquid interface
$t[s]$	Time	$bubble[-]$	Vapour bubble
$P[Pa]$	Pressure	$l[-]$	Liquid
$g[m.s^{-2}]$	Gravity acceleration	$v[-]$	Vapour
$\rho[kg.m^{-3}]$	Density	$s[-]$	Steel
$y[-]$	Mole fraction	$f[-]$	Fuel
$x[-]$	Vapour fraction	$sat[-]$	Saturation
$h[J.kg^{-1}]$	Specific enthalpy	$tot[-]$	Vapour and liquid
$\Delta h_{l,v}[J.kg^{-1}]$	Phase change specific enthalpy	$exch[-]$	Exchange
$T[K]$	Temperature	$RT[-]$	Rayleigh-Taylor
$V[m^3]$	Volume	$M[-]$	Most unstable
$Q[J]$	heat transfer	$c[-]$	Cut-off
$\varphi[W.m^{-2}.K^{-1}]$	Heat transfer coefficient	$i[-]$	Number of the family
$\lambda[m]$	Wavelength	$j[-]$	Steel or fuel
$\sigma[N.m^{-1}]$	Surface tension	$drop[-]$	Droplet
$S[m^2]$	Area	$rad[-]$	Radiative
$\epsilon[-]$	Radiative absorbtivity	$conv[-]$	Convective
$\nu[W.m^2K^{-4}]$	Stefan-Boltzmann constant	GF	Fission gases
$D_T[m]$	Core diameter		
$R[m]$	Radius in spherical geometry		

REFERENCES

1. *Les reacteurs nucleaires caloporteur sodium*, Le Moniteur, CEA Saclay (2014)

2. F. BERTRAND, *Methodologies d'etudes de surete et applications pour la pre-conception de differents types de reacteurs nucleaires de quatrieme generation*, Memoire d'habilitation a diriger des recherches de l'Universite Grenoble Alpes, CEA Cadarache (2018)

3. M. FERMIGIER and al, "Two-dimensional pattern in Rayleigh-Taylor instability of a thin layer," *Journal of Fluid Mechanics*, **236**, pp. 349 – 383 (1992)

4. D. J. LEWIS, "The instability of liquid surface when accelerated in a direction perpendicular to their planes, II," *Pro. Roy. Soc. A*, **202**, pp. 81 – 95 (1950)

5. M. L. CORRADINI, "Heat transfert and fluid flow aspects of fuel coolant interaction," COO-2781-12TR, Massachussetts Institute of Technology (1978)

6. F. LAINAULT, *Modelisation de la liberation d'energie lie aux accidents graves dans les reacteurs nucleaires a neutrons rapides*, Universite de Poitiers (1997)

7. P. MARMOTTANT, *Atomisation d'un liquide par un courant gazeux*, Institut national polytechnique de Grenoble (2001)

8. X. MANCHON and al, "Modeling and analysis of molten fuel vaporization and expansion for a sodium fast reactor severe accident," *Nuclear Engineering and Design*, **322**, pp. 522 – 535 (2017)